HHS Public Access

Author manuscript

Chem Commun (Camb). Author manuscript; available in PMC 2017 May 19.

Published in final edited form as:

Chem Commun (Camb). 2016 May 19; 52(43): 6997–7000. doi:10.1039/c6cc02764d.

Quantum Dot – NanoLuc Bioluminescence Resonance Energy Transfer Enables Tumor Imaging and Lymph Node Mapping In Vivo

Anyanee Kamkaew[a,#], **Haiyan Sun**[a,#], **Christopher G. England**[a], **Liang Cheng**[a,b], **Zhuang Liu**[b], and **Weibo Cai**[a,c]

Weibo Cai: wcai@uwhealth.org

[a]Departments of Radiology and Medical Physics, University of Wisconsin-Madison, WI 53705, USA

[b]Institute of Functional Nano & Soft Materials (FUNSOM), Collaborative Innovation Center of Suzhou Nano Science and Technology, Soochow University, Suzhou, Jiangsu 215123, China

[c]University of Wisconsin Carbone Cancer Center, Madison, WI 53705, USA

Abstract

A small luciferase protein (Nluc) was conjugated to QDs as a bioluminescence resonance energy transfer (BRET) pair. The conjugate showed 76% BRET efficiency and lymph node mapping was successfully performed. cRGD peptide was conjugated to QD-Nluc for tumor targeting. The self-illuminating QD-Nluc showed excellent energy transfer in a living system and offered optimal tumor-to-background ratio (>85).

In vivo near-infrared (NIR) fluorescence imaging (FLI) is an inexpensive, highly sensitive, and widely employed preclinical strategy for studying many diseases, including cancer.[1] However, this technique requires an external light source to excite the fluorescent molecules, which limits the tissue penetration capabilities due to the absorption and scattering of photons elicited by tissues. Therefore, it is essential to develop an imaging probe that emits light in NIR region (700 – 1000 nm) without requiring an external light source for activation. This will decrease undesired background signal and improve our imaging capabilities. Bioluminescence imaging (BLI) is a sensitive and non-invasive technique for visualizing biological processes *in vivo* using bioluminescent proteins, such as the luciferase enzyme. However, the preclinical use of BLI for in vivo applications has been limited by its weak signal intensity and short duration.[2] To solve these problems, bioluminescence resonance energy transfer (BRET)-based NIR imaging has emerged as a promising tool for non-invasively monitoring complex biological processes, including tumor growth and progression.[3]

Quantum dots (QDs) are ideal BRET acceptors due to their unique optical properties, including high quantum yield, large molar extinction coefficient, enhanced photostability,

[#]These authors contributed equally to this work

[†]Electronic Supplementary Information (ESI) available. See DOI: 10.1039/x0xx00000x

large stokes shift, and tunable surface functionalization.[4] Most BRET reporters have been constructed with *Renilla* luciferase (RLuc) and its variants, which serve as the donor molecule for different types of QDs.[5] Recently, firefly luciferase (FLuc) BRET-QD fusions have also been investigated.[6] However, these conjugations suffer from sub-optimal acceptor activation due to the poor sensitivity and suboptimal kinetics of light production.[7]

To overcome these challenges, we utilized Nano luciferase (Nluc) of the deep-sea shrimp *Oplophorus gracilirostris* for its superior brightness, enhanced pH and temperature stability, and prolonged luminescence output.[8] Previously, Nluc was shown to offer >150-fold brighter luminescence, as compared to FLuc and RLuc.[8] In this work, we developed a novel self-illuminating QD-conjugate using Nluc for *in vivo* NIR imaging. As a smaller luciferase enzyme, Nluc is optimal for conjugation to small nanoparticles such as QDs, and its enhanced luminescence potential makes it possible to obtain highly sensitive images with excellent contrast using small quantities of the imaging agent.

Preparations of QD-Nluc and QD-Nluc-cRGD

We conjugated the amino groups of Nluc (blue light emission peaking at 460 nm upon addition of its substrate furimazine, Fig. 1b) to carboxylates presented on the polymer-coated CdSe/ZnS core-shell QD705 (fluorescent emission peaking at 705 nm, Fig. 1b) through carbodiimide-mediated amide coupling. For tumor targeting, cyclic arginine-glycine-aspartic acid peptides (cRGD) were selected for their strong affinity for integrin $\alpha_v\beta_3$, known to be expressed in many tumor types.[9] Moreover, the small size of cRGD peptides makes them well-suited for conjugation to QDs. Nluc was incubated with QD705 for 1 h before cRGD peptides were added to the mixture continue with shaking for 1 h (Fig. 1a). Gel electrophoresis analysis showed bands with different mobility, confirming successful conjugation (Fig. 1d). The average sizes of conjugates were measured by dynamic light scattering and were 32.3 ± 4.8 nm and 36.3 ± 0.7 nm for QD-NLuc and QD-Nluc-cRGD, respectively compared to 21.2 ± 2.5 nm for unconjugated QD (Fig. S1a–c). The protein (Nluc) concentration of each sample was determined by Bradford protein assay, and the concentration of QD705 was spectrophotometry calculated via Beer's law.

The bioluminescence emission of QD-Nluc was measured upon addition of furimazine (Fig. 1c). In addition to the emission of Nluc peaking at 460 nm, a strong peak at 705 nm was also detected, indicating the efficiency of BRET. The BRET ratio was determined to be 13.3, which corresponded to 76% BRET efficiency.[10] The conjugates were stable in serum and phosphate buffer saline (PBS) after storage at 4°C for 30 days (Fig. S1d).

Lymphatic imaging with QD-Nluc

Sentinel lymph node (SLN) mapping is one of the most promising cancer-related applications since these nodes are typically the first to develop lymphatic metastases.[11] There are several imaging strategies for lymph node mapping; however, many of these imaging approaches are limited. For example, the blue dye injection suffers from minimal tissue penetration,[12] lymphoscintigraphy has low spatial resolution and requires exposure to radioactivity,[13] and SPECT/CT requires radioactive tracers and long acquisition times.[14]

Therefore, optical imaging is a promising modality for visualizing the lymph node system, with regards to image quality and operational cost. For example, indocyanine green is an FDA-approved fluorophore that has been widely used as an NIR fluorescence imaging agent for detection of lymph nodes and tumors in clinical trials.[15]

Herein, we demonstrate that our QD-Nluc conjugate may be employed for lymph node mapping. The conjugate was intradermally injected into the hind paw before furimazine was intravenously injected. Strong bioluminescence and BRET signals in the popliteal (PO) lymph node were visualized at 5 min post-injection (p.i.), devoid of any background signal (Fig. 2a). Sufficient signal for imaging was observed for >2 h after a single substrate injection, allowing for visualization of two more lymph nodes (PO and iliac, Fig. 2a). Similarly, lymph nodes were clearly visualized by bioluminescence and BRET when the QD-Nluc conjugate was introduced into all four paws (Fig. S2). The lymph nodes were removed for *ex vivo* NIR FLI and the results validated the BLI (Fig. 2b). Finally, confocal imaging of lymph node tissues confirmed the high accumulation of nanoconjugate in the lymph node (Fig. 2c) as compared to the control lymph node (Fig. 2d).

Tumor imaging with QD-Nluc-cRGD

To demonstrate the tumor-targeting capabilities of QD-Nluc-cRGD in living animals, high integrin $\alpha_v\beta_3$-expressing U87MG human glioblastoma cells were employed as this receptor plays a vital role in tumor angiogenesis and metastasis.[16] In this study, the target and non-target conjugates were incubated with U87MG cells for 3 h then imaged using confocal microscopy. A strong NIR fluorescent signal was observed from the cells incubated with targeting material (Fig. 3a), while minimal NIR fluorescence was detected in cells incubated with QD-Nluc (Fig. 3b) or without any nanomaterials (Fig. 3c). Next, the energy transfer process was demonstrated in live cells. U87MG cells were incubated with QD-Nluc and QD-Nluc-cRGD for 30 min on ice. After washing thoroughly, furimazine was added to the cells solutions and the bioluminescence and BRET signals were visualized with no filter (to collect the emission from Nluc and QD705) and with an emission filter of 690–710 nm (to collect only QD705 emission, Fig. 3d). Cells imaged both with and without the filter showed brilliant BL from the cells containing RGD conjugate (2, Fig. 3d), whereas minimal signal was observed in cells lacking cRGD (1, Fig. 3d). These results suggest that BRET between Nluc and QD705 is highly stable and can occur in live cells without eliciting any toxicity (Fig. 3e). Also, additional cell lines were examined for potential toxicities (Fig. S3).

The QD-Nluc with and without cRGD conjugates were intravenously injected (~ 20 pmol of QD, ~ 8.5 μg of NanoLuc) into U87MG tumor-bearing mice. Mice were imaged multiple times after injection using the IVIS200^{TM} system (Fig. 4). The *in vivo* fluorescence signals of the conjugates were collected with an emission filter (690–710 nm) and an excitation filter of 450–480 nm (Fig. 4a and 4b). Enhanced fluorescence signal was observed in the tumor mice injected with QD-Nluc-cRGD as early as 5 min p.i. and remained high for 30 min p.i. (Fig. 4a) before gradually decreasing. Region-of-interest measurements showed tumor-to-background ratios (TBRs) from the targeting group (QD-Nluc-cRGD) were 4.2 ± 0.3 (5 min), 2.6 ± 0.1 (30 min), 2.1 ± 0.1 (1 h), and 1.7 ± 0.3 (2 h), where the background refers to region surrounded tumor, $n = 3$ (Fig. S4a). A weak fluorescence signal was

observed in the tumor of QD-Nluc injected mice (Fig. 4b) which was attributed to enhanced permeability and retention (EPR) effect elicited by solid tumors (TBRs were 1.8 ± 0.4 (5 min), 1.4 ± 0.1 (30 min), 1.4 ± 0.2 (1 h), and 1.0 ± 0.1 (2 h), $n = 3$; Fig. S4). There was significant fluorescence signal from the skin after 2 h p.i., which interfered with the signal from the tumor; however, this problem was resolved by monitoring the signal via bioluminescence with no excitation light (Fig. 5a and 5b).

BLI was conducted in the same mouse since QD-Nluc conjugates offer simultaneous FLI and BLI. The bioluminescence signal was much stronger than the fluorescence one, especially at 2 h p.i. in the mouse injected with QD-Nluc-cRGD (Fig. 5b).

Under no filter, the TBRs were 102.3 ± 9.1 (5 min), 74.6 ± 1.8 (30 min), 61.3 ± 1.0 (1 h), and 23.0 ± 3.1 (2 h), $n = 3$ (Fig. S4b). Intense luminescence signal was still observed after using an emission filter validating the BRET efficiency *in vivo* (Fig. 5b), and the TBRs were 90.7 ± 6.3 (5 min), 37.8 ± 2.7 (30 min), 30.9 ± 5.2 (1 h), and 10.6 ± 1.0 (2 h), $n = 3$ (Fig. S4b). Passive targeting of QD-Nluc was better visualized via BLI; however, the TBRs were significantly lower than the ones obtained from active targeting group (data obtained without using any filter, Fig. S4c). These results reveal that BLI displays higher sensitivity for *in vivo* cancer imaging, as compared to FLI.

Finally, mice injected with QD-Nluc and QD-Nluc-cRGD were sacrificed at 2 h p.i. and organs were harvested and imaged immediately. *Ex vivo* imaging revealed that most nanoparticles accumulated in the liver for both cases (with and without cRGD, Fig. 6a). However, the QD signal is noticeably visible in the U87MG tumors of mice injected with QD-Nluc-cRGD, confirming the active targeting capabilities of nanoparticles functionalized with cRGD peptides (Fig. 6b). To validate the tumor-specific uptake of QD-Nluc-cRGD, tumor tissue was cryosectioned and stained with DAPI to visualize cell nuclei (Fig. 6c and 6d). A stronger QD fluorescence signal was observed in the tumor sections from mice injected with QD-Nluc-cRGD (Fig. 6d) compared to the one with QD-Nluc (Fig. 6c). These results confirmed that QD-Nluc-cRGD specifically accumulated in U87MG tumors.

For animal imaging, BLI provides exceptionally higher sensitivity than FLI. In BRET, the energy transfer process will result in the loss of some luminescence with the distance between the donor (*i.e.* Nluc) and acceptor (*i.e.* QD705) influencing the BRET ratio.[5a] In this study, Nluc was directly conjugated to the QD without any further surface modification to avoid BRET signal reduction. Nluc offers an improved performance of BRET assays due to its small size (19 kDa) which increases the donor to acceptor ratio. Moreover, the luminescence of furimazine (an evolved coelenterazine derivative) is >30-times brighter than coelenterazine.[8] In addition, the bioluminescence spectrum for Nluc is narrower than Rluc8, allowing for better spectral discrimination with acceptor fluorophores which is useful for cases that utilize green or yellow-emitting fluorophores.[17]

Herein, we successfully demonstrated the efficient visualization of the lymphatic system using QD-Nluc conjugates with bioluminescence and BRET-based imaging modalities, which offered enhanced brightness and higher contrast in comparison to FLI techniques. BLI of tumor-bearing mice injected with QD-Nluc-cRGD provided exceptionally high TBRs

>85 in both cases, with and without emission filter. The luminescent signal was clearly visible at 5 min p.i. of the conjugate and furimazine substrate. Moreover, BRET signal remained high and slowly decayed, closely resembling the half-life of Nluc *in vivo*, indicating that the conjugate remained stable.

To the best of our knowledge, this is the first report of Nluc-conjugated QDs for BRET-based imaging *in vivo*. Nluc is an ideal BRET donor for QDs due to its small size and enhanced luminescence output. The energy transfer appeared to be more efficient compared to the similar QD-BRET conjugate using Rluc8.[5a] The combination of Nluc and other acceptors can be tuned for appropriate study. For future studies, the advantages of Nluc can also be applied to other systems such as deep-tumor photodynamic therapy[18] and deep-tissue protein-protein interaction study in living systems.[7b, 19]

Supplementary Material

Refer to Web version on PubMed Central for supplementary material.

Acknowledgments

This work is supported, in part, by the University of Wisconsin-Madison, the National Institutes of Health (NIBIB/NCI 1R01CA169365, P30CA014520, T32CA009206), and the American Cancer Society (125246-RSG-13-099-01-CCE). We thank Promega Corporation for their generous gifts of NanoLuc and furimazine.

Notes and references

1. Hilderbrand SA, Weissleder R. Curr Opin Chem Biol. 2010; 14:71–79. [PubMed: 19879798]
2. Badr CE. Methods Mol Biol. 2014; 1098:1–18. [PubMed: 24166364]
3. (a) De A. Curr Pharm Biotechnol. 2011; 12:558–568. [PubMed: 21342101] (b) Xia Z, Rao J. Curr Opin Biotechnol. 2009; 20:37–44. [PubMed: 19216068]
4. (a) Michalet X, Pinaud FF, Bentolila LA, Tsay JM, Doose S, Li JJ, Sundaresan G, Wu AM, Gambhir SS, Weiss S. Science. 2005; 307:538–544. [PubMed: 15681376] (b) Mattoussi H, Palui G, Na HB. Adv Drug Deliver Rev. 2012; 64:138–166.
5. (a) So MK, Xu C, Loening AM, Gambhir SS, Rao J. Nat Biotechnol. 2006; 24:339–343. [PubMed: 16501578] (b) Yao H, Zhang Y, Xiao F, Xia Z, Rao J. Angew Chem Int Ed Engl. 2007; 46:4346–4349. [PubMed: 17465433] (c) Xiong L, Shuhendler AJ, Rao J. Nat Commun. 2012; 3:1193. [PubMed: 23149738]
6. (a) Alam R, Fontaine DM, Branchini BR, Maye MM. Nano Lett. 2012; 12:3251–3256. [PubMed: 22620681] (b) Alam R, Zylstra J, Fontaine DM, Branchini BR, Maye MM. Nanoscale. 2013; 5:5303–5306. [PubMed: 23685756] (c) Alam R, Karam LM, Doane TL, Coopersmith K, Fontaine DM, Branchini BR, Maye MM. ACS Nano. 2016; 10:1969–1977. [PubMed: 26760436]
7. (a) De A, Loening AM, Gambhir SS. Cancer Res. 2007; 67:7175–7183. [PubMed: 17671185] (b) Dragulescu-Andrasi A, Chan CT, De A, Massoud TF, Gambhir SS. Proc Natl Acad Sci U S A. 2011; 108:12060–12065. [PubMed: 21730157] (c) Saito K, Chang YF, Horikawa K, Hatsugai N, Higuchi Y, Hashida M, Yoshida Y, Matsuda T, Arai Y, Nagai T. Nat Commun. 2012; 3:1262. [PubMed: 23232392]
8. Hall MP, Unch J, Binkowski BF, Valley MP, Butler BL, Wood MG, Otto P, Zimmerman K, Vidugiris G, Machleidt T, Robers MB, Benink HA, Eggers CT, Slater MR, Meisenheimer PL, Klaubert DH, Fan F, Encell LP, Wood KV. ACS Chem Biol. 2012; 7:1848–1857. [PubMed: 22894855]
9. (a) Danhier F, Le Breton A, Preat V. Mol Pharm. 2012; 9:2961–2973. [PubMed: 22967287] (b) Chen K, Chen X. Theranostics. 2011; 1:189–200. [PubMed: 21547159]
10. Pfleger KD, Eidne KA. Nat Methods. 2006; 3:165–174. [PubMed: 16489332]

11. (a) Pelosi E, Ala A, Bello M, Douroukas A, Migliaretti G, Berardengo E, Varetto T, Bussone R, Bisi G. Eur J Nucl Med Mol Imaging. 2005; 32:937–942. [PubMed: 15838690] (b) Agarwal A, Heron DE, Sumkin J, Falk J. J Surg Oncol. 2005; 92:4–8. [PubMed: 16180213]
12. Ahmed M, Purushotham AD, Horgan K, Klaase JM, Douek M. Br J Surg. 2015; 102:169–181. [PubMed: 25511661]
13. Spillane AJ, Noushi F, Cooper RA, Gebski V, Uren RF. Ann Oncol. 2009; 20:977–984. [PubMed: 19153113]
14. Vercellino L, Ohnona J, Groheux D, Slama A, Colletti PM, Chondrogiannis S, Merlet P, Toubert ME, Rubello D. Clin Nucl Med. 2014; 39:431–436. [PubMed: 23877520]
15. (a) Schaafsma BE, Mieog JS, Hutteman M, van der Vorst JR, Kuppen PJ, Lowik CW, Frangioni JV, van de Velde CJ, Vahrmeijer AL. J Surg Oncol. 2011; 104:323–332. [PubMed: 21495033] (b) Hirche C, Engel H, Hirche Z, Doniga S, Herold T, Kneser U, Lehnhardt M, Hunerbein M. Ann Plast Surg. 2014; 73:701–705. [PubMed: 23782892] (c) Plante M, Touhami O, Trinh XB, Renaud MC, Sebastianelli A, Grondin K, Gregoire J. Gynecol Oncol. 2015; 137:443–447. [PubMed: 25771495]
16. Desgrosellier JS, Cheresh DA. Nat Rev Cancer. 2010; 10:9–22. [PubMed: 20029421]
17. (a) Schaub FX, Reza MS, Flaveny CA, Li W, Musicant AM, Hoxha S, Guo M, Cleveland JL, Amelio AL. Cancer Res. 2015; 75:5023–5033. [PubMed: 26424696] (b) Machleidt T, Woodroofe CC, Schwinn MK, Mendez J, Robers MB, Zimmerman K, Otto P, Daniels DL, Kirkland TA, Wood KV. ACS Chem Biol. 2015; 10:1797–1804. [PubMed: 26006698]
18. Kim YR, Kim S, Choi JW, Choi SY, Lee SH, Kim H, Hahn SK, Koh GY, Yun SH. Theranostics. 2015; 5:805–817. [PubMed: 26000054]
19. (a) Xu X, Soutto M, Xie Q, Servick S, Subramanian C, von Arnim AG, Johnson CH. Proc Natl Acad Sci U S A. 2007; 104:10264–10269. [PubMed: 17551013] (b) Pfleger KD, Seeber RM, Eidne KA. Nat Protoc. 2006; 1:337–345. [PubMed: 17406254]

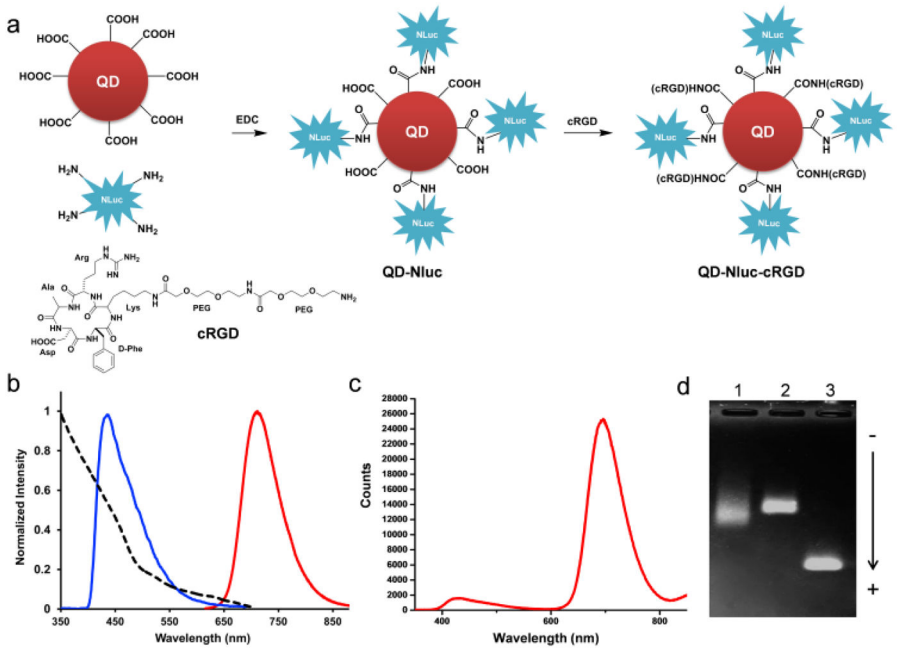

Fig. 1.

Characterization of bioluminescent-QD conjugates based on BRET. (a) Synthesis of QD-Nluc and QD-Nluc-cRGD conjugates. (b) Absorption and emission spectra of QD705 (λ_{ex} = 465 nm), and bioluminescence of furimazine catalyzed by Nluc. (c) Bioluminescence emission spectrum of QD-Nluc in PBS. (d) Gel electrophoresis analysis of the conjugates; lane 1 is purified QD-Nluc conjugate; lane 2 is purified QD-Nluc-RGD conjugate, and lane 3 is unconjugated QD705.

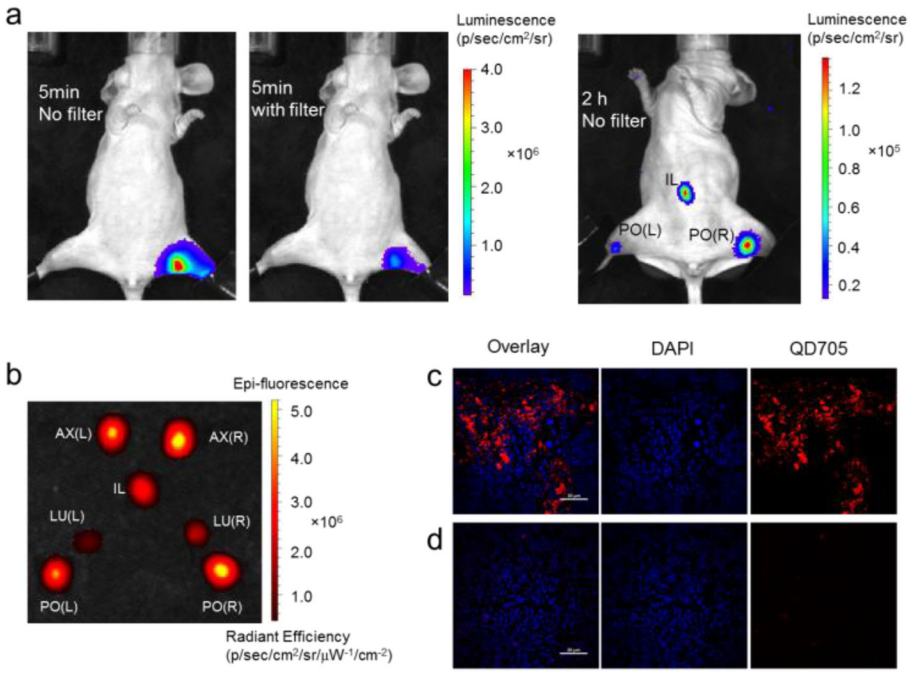

Fig. 2.

In vivo luminescence lymph node imaging. (a) Bioluminescence imaging of lymphatic basins in a mouse injected with QD-Nluc intradermally in a hind paw. (b) Fluorescence image of lymph nodes excised from the mouse injected with QD-Nluc in four paws (see Fig. S2); L, left; PO, popliteal lymph node; LU, lumbar lymph node; IL, iliac; AX, axillary lymph node; R, right. (c–d) Histological images of lymph node slices from a mouse in (a); (c) PO lymph node from injected mouse exhibited bright signal from QD705 (red) whereas no significant emission from QD705 was observed in PO lymph node from non-injected mouse (d). DAPI (blue) represents nuclease, scale bar: 20 μm.

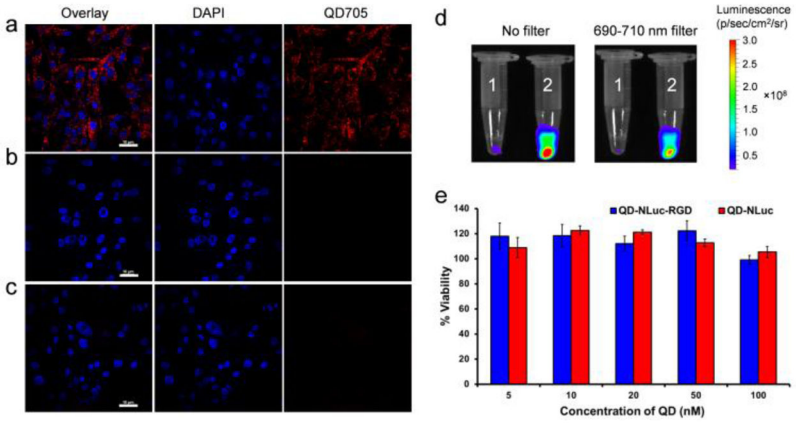

Fig. 3.

Fluorescence and luminescence imaging of U87MG cells with QD-Nluc-cRGD conjugate. (a–c) Confocal imaging; (a) cells were incubated with QD-Nluc-cRGD for 3 h, (b) cells were incubated with QD-Nluc for 3 h and (c) control cells without any conjugates, scale bar: 10 μm. (d) Luminescence images of labeled cells acquired without any filter (left) and with a filter (690–710 nm, right); cells were incubated with QD-Nluc (tube 1) and QD-Nluc-cRGD (tube 2). (e) Cell viability of U87MG cells evaluated by MTT assay in a dose-dependent manner of QD-Nluc and QD-Nluc-cRGD conjugates. Data represent mean ± s.d. ($n = 4$).

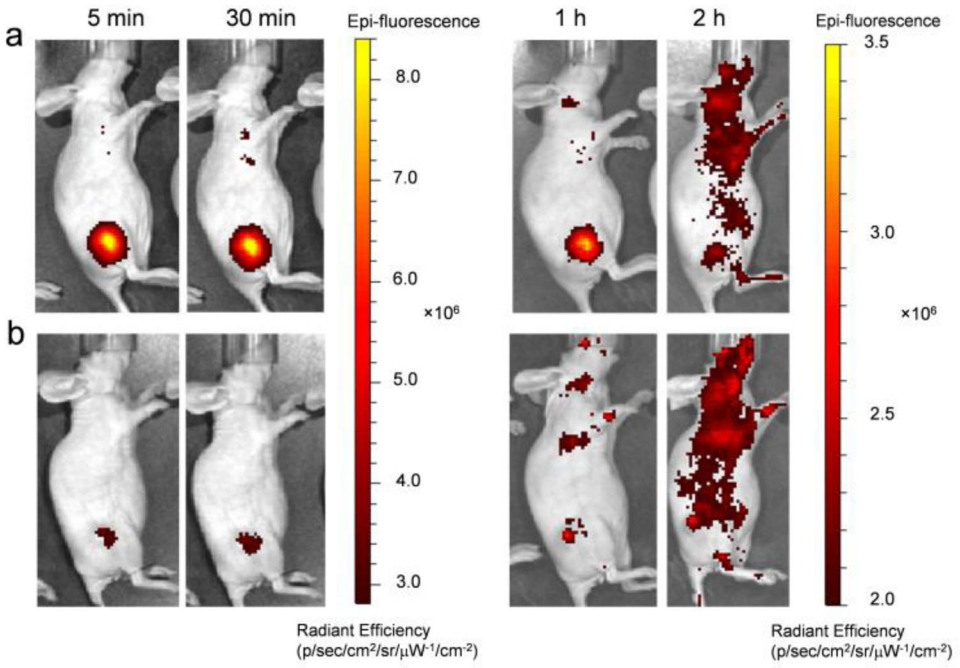

Fig. 4.

In vivo fluorescence imaging of U87MG tumor-bearing mice. (a,b) Time-dependent fluorescence imaging of U87MG tumor-bearing mouse intravenously injected with (a) QD-Nluc-cRGD or (b) QD-Nluc at 5 min, 30 min, 1 h and 2 h p.i..

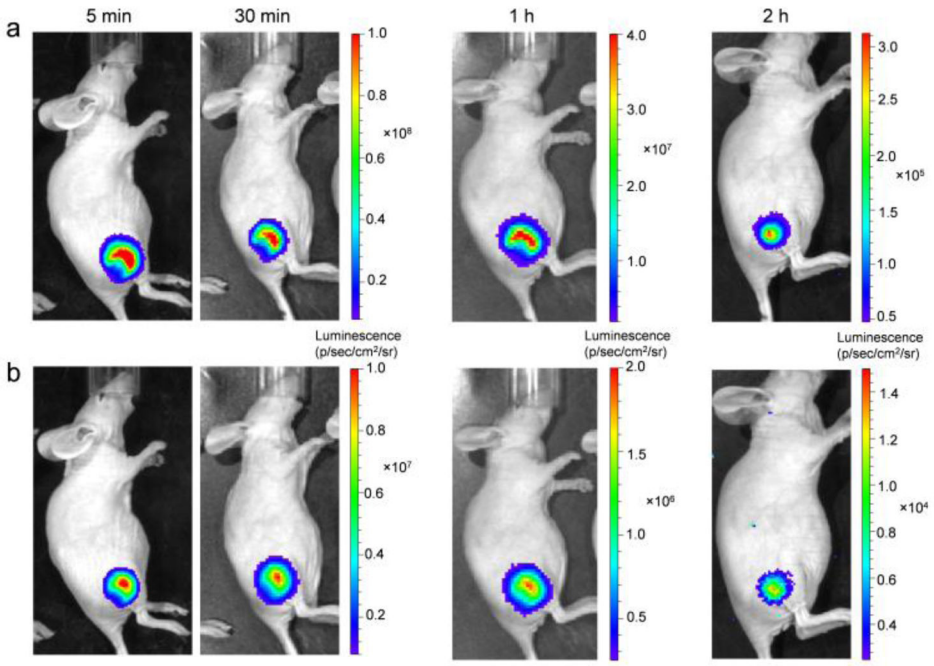

Fig. 5.

Luminescence imaging of U87MG tumors in mice with QD-Nluc-cRGD. a,b) Time-dependent bioluminescence imaging of U87MG tumor-bearing mouse intravenously injected with QD-Nluc-cRGD (the same mouse as Fig. 4a) and single injection of furimazine substrate. Images in a) acquired without any emission filter with acquisition time: 1 s (5 min), 1 s (30 min), 1 s (1 h) and 10 s (2 h). Images in b) acquired with emission filter (690–710 nm) with acquisition time: 10 s (5 min), 10 s (30 min), 30 s (1 h) and 3 min (2 h).

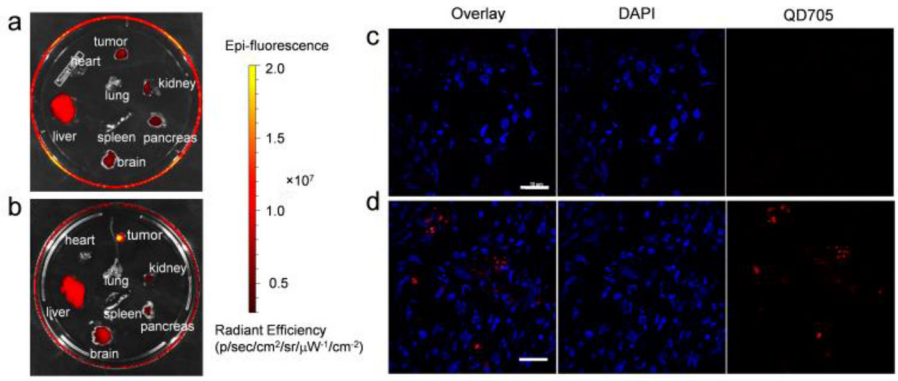

Fig. 6.

Ex vivo fluorescence imaging of organs and tumor tissues. a,b) Fluorescence images of organs excised from the mice in Fig. 4 injected with QD-Nluc (a) and QD-Nluc-cRGD (b). c,d) Histology of frozen U87MG tumors slices from a mouse injected with QD-Nluc (c) and QD-Nluc-cRGD (d). Scale bar: 10 μm.